Simulation of FMCW Radar Systems Based on Software Defined Radio

Carlos López-Martínez CARLOS.LOPEZ@TSC.UPC.EDU
Universitat Politècnica de Catalunya UPC, Signal Theory and Comms. Dept., Jordi Girona 1-3, 08034 Barcelona, SPAIN

Marc Vidal-Morera MARCVIDAL93@GMAIL.COM
Universitat Politècnica de Catalunya UPC, Signal Theory and Comms. Dept., Jordi Girona 1-3, 08034 Barcelona, SPAIN

Abstract

This work address the implementation of a Frequency Modulated Continuous Wave radar based on Software Defined Radio. In particular, we have simulated a USRP device implementing the radar system, in order to determine the radar performances, specially in terms of achievable range and range spatial resolution. We have considered the Ettus system X300/X310 equipped with a UBX 10-6000 MHz Rx/Tx daughterboard. The different simulation demonstrate that the radar would achieve a range of $3Km$ with a range resolution in the order of $10m$. Additional simulations at different carrier frequencies detail the achievable radar performances.

1. Introduction

The initial aim of the work presented in this paper is to develop a Synthetic Aperture Radar (SAR) based on the Software Defined Radio (SDR) technology. SAR systems, also known as microwave imaging systems, can be classified as active microwave systems (Curlander & McDonough, 1991). During the last decades, they have demonstrated their usefulness for Earth observation, as their imaging capabilities are weather and illumination independent, being also able to provide high spatial resolution information of the observed area. When boarded on orbital platforms, they allow a global monitoring being able to address universal problems that may affect the humankind, as for instance, global warming.

In a first period, covering since its conception in the 50s to early 90s, SAR systems were characterized by presenting a single-channel nature and being boarded mainly on orbital platforms. Nevertheless, from the early 90s, the SAR technology shows its full potential thanks to the emergence of multi-channel SAR techniques: SAR interferometry (InSAR) (Bamler et al., 1998), SAR polarimetry (PolSAR) (Ulaby & Elachi, 1990; Cloude & Pottier, 1996) and the combination of both in polarimetric SAR interferometry (PolInSAR) (Cloude & Papathanassiou, 1998). As demonstrated, multidimensional SAR systems allow the estimation of a large number of geophysical and biophysical characteristics of the Earth's surface. Since the 90s, SAR systems started to operate also on board airplanes, enabling a cost reduction and also allowing to focus on particular areas of the Earth's surface. Both, orbital and airborne SAR systems, despite their importance, have important limitations in cases where great flexibility in terms of temporal revisit, i.e., when it is necessary to observe the same target with a high temporal frequency or even by a continuous observation. In the case of orbital systems, considering a single satellite, it is impossible to observe the same area in less than two or three times a month due to the limitations of the satellite orbit. This limitation could be partially solved by airborne systems, but with a prohibitive cost.

In order to overcome the previous limitations, in recent years, the design of terrestrial SAR systems or Ground Based SAR (GBSAR) systems has emerged (A. et al., 2004; Rudolf et al., 1999; Tarchi, 1999). The main difference of these systems is that they allow greater flexibility to monitor a target with a high temporal flexibility, also characterized by its ease of deployment and much lower cost. The high stability of the terrestrial platform and flexibility in terms of revisit time make such systems ideal for monitoring and detecting changes in local areas of interest with high spatial resolution and a temporal resolution of minutes. In addition, the terrestrial geometry allows to address some intrinsic limitations of orbital geometries. In this context, the first GBSAR systems were developed based on vector network analysers or VNAs. The use of VNA systems allows versatility in signal generation and the development of a GBSAR system without the need for a complex electronic development of microwave systems. However, this type of solution has the major drawback of requiring a long acquisition time for a single SAR image. In the case of a GBSAR system, the acquisition time of an image should be minimized to avoid distortions that may negatively impact on the quality of the final image.

Proceedings of the 6^{th} GNU Radio Conference, Copyright 2016 by the author(s).

In order to reduce the acquisition time of an image, GB-SAR systems are nowadays designed as radars based on frequency modulated continuous signals in FMCW (Frequency Modulation Continuous Wave) architecture. The use of this architecture may reduce the acquisition time of an image and therefore improve its quality. In addition, the flexibility of these systems makes the acquisition of images in interferometric or polarimetric modes possible. The main limitation of this type of solution is that the complete design and development of the radar system hardware is necessary, resulting in a high cost and design time.

With the aim to overcome the limitations of the design of current GBSAR systems, the idea presented in this paper is to develop a SAR system based on SDR technology. Due to the technical complexity of a SAR system, both in hardware and software terms, we developed a simpler FMCW radar system based on SDR technology. In order to have a complete characterization of this type of system, we have created a simulator of a FMCW radar system based on SDR technology, similarly to (Elsner et al., 2009) The idea to develop this simulator was twofold. On the one hand, to be able to determine the performances of a radar system. On the other hand, to test the different architectures that could be employed to obtain a FMCW radar system based on SDR technology.

This work is divided as follows. Section 2 describes the principles of a FMCW radar. Section 3 presents the design of the simulator which is presented in Section 4. The different results of the simulator are presented in Section 5. The final conclusions are presented in Section 6.

2. FMCW Radars

In case of spaceborne and airborne SAR systems, these consist on pulsed radars. Nevertheless, in the case of terrestrial SAR sensors, these type of systems can not be employed as the energy received and scattered back by the target of interest would be very low, leading to a very low Signal-to-Noise ratio. In order to increase the Signal-to-Noise ratio, FMCW architectures are desirable for short range radar and SAR systems. Fig. 1 details the basic architecture of a FMCW radar system.

As it can be observed, the transmitting block consists of a signal generator that creates a frequency modulated signal on the basis of a carrier frequency $f_0(t)$. SAR and radar systems for Earth observation operate in frequencies that range from 0.5 to $10GHz$, being the most important ones: $435MHz$ (P band), $1.2GHz$ (L band), $5.2GHz$ (C band) and $9.6GHz$ (X band). The selection of the carrier frequency depends on the properties of the Earth surface that want to be estimated. For instance, low frequencies (P and L band) are employed when penetration into the vegetation

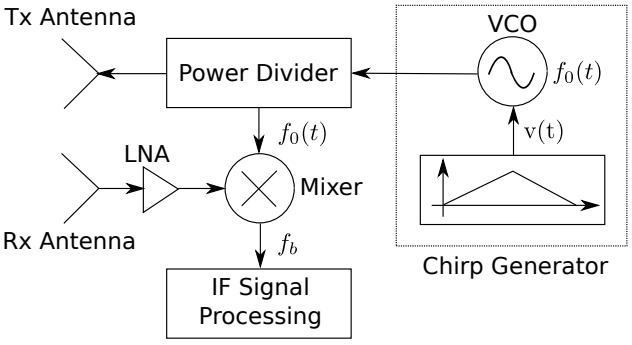

Figure 1. FMCW radar system architecture.

is desired. The carrier frequency is linearly modulated in frequency leading to the transmitted pulse, also known as chirp signal,

$$p(t) = \prod \left(\frac{t - T_p/2}{T_p} \right) e^{j\beta t + j\alpha t^2}. \quad (1)$$

where $\beta = 2\pi f_0$. Fig. 2 details the instantaneous frequency of the frequency modulated pulse in Eq. 1, where α represents the chirp rate.

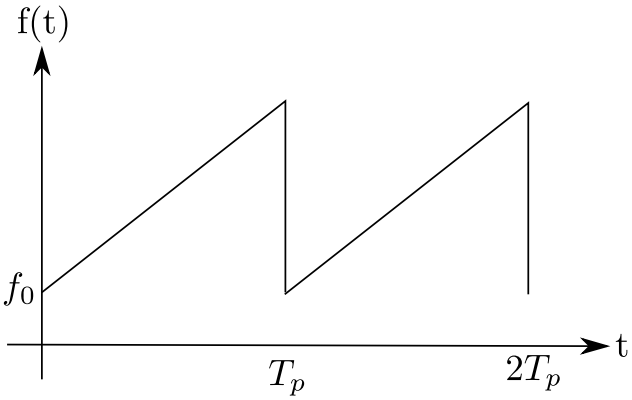

Figure 2. Chirp signal instantaneous frequency.

The transmitted pulse in Eq. 1 reaches a set of N targets that are characterized by the complex reflectivity function

$$\Gamma(t) = \sum_{i=1}^{N} \sqrt{\sigma_n} e^{j\phi_n} \delta(t - t_n) = \sum_{i=1}^{N} \sqrt{\sigma_n} e^{j\phi_n} \delta\left(t - \frac{2r_n}{c}\right) \quad (2)$$

.

where c represents the speed of light. A generic point target n at a range distance r_n from the radar is characterized by a

radar cross section σ_n (RCS) and a phase ϕ_n. Finally, t_n is the round trip delay. The received signal corresponds to the convolution of the transmitted pulse in Eq. 1 with the complex reflectivity function in Eq. 2. In order to obtain the information of interest of the different targets, that is, their range positions, the received signal is mixed with a sample of the transmitted one in a mixer. This process is also known as deramping process. From a mathematical point of view, it consists on multiplying the conjugated received signal by the phase term of the transmitted chirp

$$s_c(t) = s^*(t) * e^{j\beta t + j\alpha t^2 = \sum_{i=1}^{N} \sqrt{\sigma_n} e^{j\phi_n}} \cdot \prod \left(\frac{t-(T_p/2+t_n)}{T_p} \right) e^{j(\beta t_n - \alpha t_n^2)} e^{j2\alpha t_n t} \quad (3)$$

The terms related to the round-trip delay and weighted by the carrier β and by the chirp-rate α introduce an absolute phase offset, while the information concerning the target position is carried by the sinusoid $e^{j2\alpha t_n t}$. In other words, after the mixing process, the target position is encoded as the frequency of the intermediate frequency or beat frequency $f_b = \alpha t_n$. Hence, the position of the target is obtained as $r_n = (f_b/\alpha)c$.

Another parameter of interest to analyse is the spectral bandwidth Δf_b, as it determines the final range resolution of the radar Δr, that is, the capability to detect two close targets in range as different targets. It can be demonstrated that the spectral bandwidth is

$$\Delta f_b = \frac{1}{T_p - 2t_n}. \quad (4)$$

The range resolution is obtained as

$$\Delta r = \frac{\Delta f_b c T_p}{2BW} \approx \frac{c}{2BW} \quad (5)$$

where $2T_n << T_p$ has been considered, T_p period of the chirp signal, BW signal bandwidth and $2t_n$ is the round trip delay. As it can be observed, without considering the final approximation, the range resolution depends on the position of the target in such away that the further the target the worst the spatial resolution. Fig. 3 details an example of the degradation of the range resolution with respect to the range distance.

3. Simulator Design

As detailed, the main goal is to simulate a FMCW radar system based on SDR devices in order to determine the potential capabilities of a system of this type. The core idea of this simulator is to simulate a Universal Software Radio Peripherial USPR developed by Ettus Research LLC. In particular, this work is focused in the simulation of

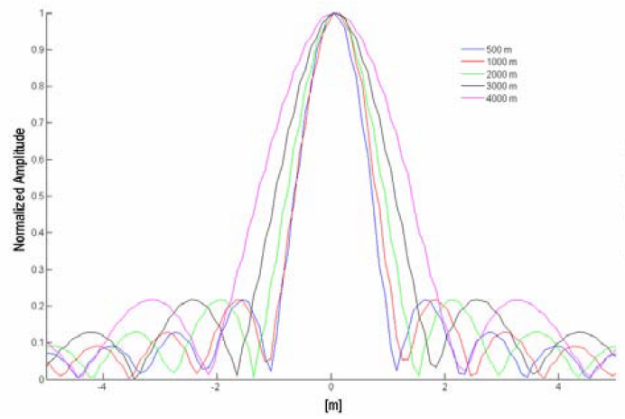

Figure 3. Retrieved space responses for targets located at different range positions.

the X300/X310 device equipped with UBX 10-6000 MHz Rx/Tx daughterboard as its capabilities, specially in terms of bandwidth, are suitable for the development of a FMCW radar system.

To make an accurate design of the simulator, it is necessary to specify the most important parameters of the FMCW radar system. Therefore, the following characteristics have been considered:

1. Carrier frequencies f_0: The carrier frequency can be selected among the following values: 500 MHz, 1.2 GHz, 5.2 GHz and 9.1 GHz. Despite the X300/X310 device is not able to generate the last carrier frequency, it is included due to its importance in different Earth observation applications.
2. System bandwidth: From $20MHz$ to $160MHz$.
3. Transmitted signal: chirp.

In order to determine the different requirements and specifications of the FCMW radar system, it is necessary to consider the radar equation that determines the received power

$$P_r = \frac{P_t G_t G_r \lambda^2 \sigma}{(4\pi)^3 r^4} \quad (6)$$

and the minimum Signal-to-Noise ratio in reception

$$SNR_{min} = \frac{P_t G_t G_r \lambda^2 \sigma}{(4\pi)^3 r^4 K T_0 2BW F L}. \quad (7)$$

Table 1 details the different parameters of the previous equations,where P refers to power, G to the antenna gain, λ to the wavelength, K is the Boltzmann constant, T is the

Table 1. Transmission and reception parameters.

Freq. [GHz]	0.5	1.2	5.2	9.1
SNR [dB]	10	10	10	10
λ [m]	0.6	0.25	0.05	0.03
P_t [dBm]	22	22	12.98	7
F [dB]	3	4	6	8
G_t, G_r [dB]	6	6	20	20
r [km]	0-3			
L [dB]	4			
K [J/K]	1.38e-23			
BW [MHz]	20-160			

ambient temperature, F the noise figure and L represents additional losses.

Respect to the antennas, the ones that have been considered in this study are manufactured by the company A-Info. In order to cover the complete frequency range from 0.5 to $9.1GHz$, three antennas are considered as detailed in Table 2.

Table 2. Antennas information.

Company	A-Info	A-Info	A-Info
Model	DS-40200	LB-187-20	LB-90-20
Type	Log Per.	Horn	Horn
Freq. rg. $[GHz]$	0.1-4	3.95-5.85	8.2-12.4
Gain [dB]	6	20	20
Size [mm] W x H x L	412x378	274x212x350	138x107x200

3.1. Spatial Resolution

The spatial resolution in the range dimension is one of the most important parameters of the radar performances, as it determines the minimum separation between two targets to be detected as separated.

As indicated in Eq. 5, the range spatial resolution depends directly on the signal bandwidth and also on the distance to the target being imaged. Considering that the mixing process in reception is performed digitally in the receiving system, Fig. 4 represents the achievable resolutions for different bandwidths and target distances. As it can be observed, the curves for close targets (below $1Km$) achieve reasonable resolutions, below $10m$, for signal bandwidths starting at $20MHz$. This is not the case for distant targets, as in order to achieve a range resolution below $10m$, larger bandwidths are necessary. In any case, a system based on a X300/X310 device equipped with a UBX 10-6000 MHz Rx/Tx daughterboard would achieve a spatial resolution below $10m$ for targets up to $3Km$. These performances can be considered at the same level of most GBSAR sensors developed nowadays.

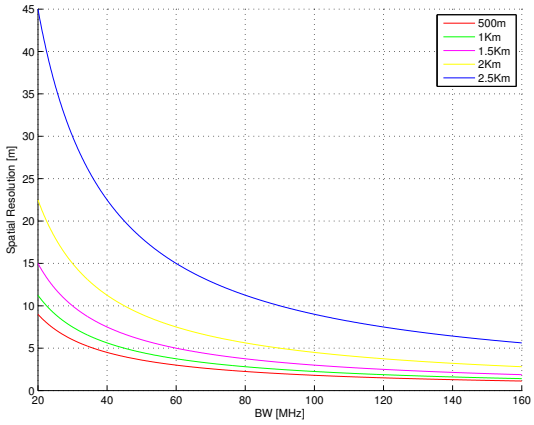

Figure 4. Spatial resolution in the range dimension.

3.2. Received Power

The received power in a radar system determines the capability of the radar to detect a particular target above the noise signal. If the received power is too low, the target will be not detected. As indicated by Eq. 6, the received power is determined according to the values specified in Table 1. Among the different parameters, it is important to specify the Radar Cross Section σ that determines the target amplitude. In this case we will consider a trihedral with $2.41m$ side (Curlander & McDonough, 1991). This is a canonical target employed in radar calibrations and it presents approximately to the target amplitude of a medium car. Fig. 5 details the different received powers for target up to $3Km$ away from the radar and at the different working frequencies.

As it can be observed, the losses in a radar system are important due to the effect of the term r^4. Consequently, the receiving system must be characterized by a high sensitivity, that in part can be solve by employing high gain antennas. Despite this solution is acceptable in the case of a simple FMCW radar, when addressing a SAR system, this can not be considered as high beam width antennas, that is low gain antennas, are necessary. Consequently, a receiving system with a high sensitivity is mandatory.

3.3. Detectable RCS

The previous section considered the received power by the radar system. This parameter, considering the SNR established in Table 1, can be employed to determine the minimum detectable Radar Cross Section σ. Fig. 6 details the

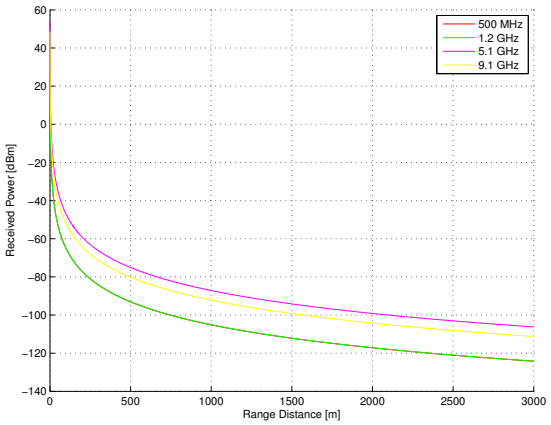

Figure 5. Received power considering $BW = 120MHz$.

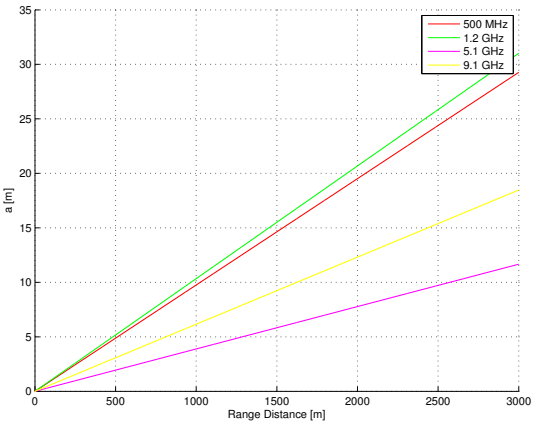

Figure 7. Trihedral dimension according to the RCS in Fig. 6.

values of the RCS for different target distances and at different frequencies. These plots have been calculated considering the parameters in Table 1. As it can be observed, the more distant the target, the largest its RCS in order to be detected.

This RCS can be transformed into target dimensions, when considering a canonical trihedral. Fig. 7 shows the side dimension of the trihedral giving the RCS detailed in Fig. 6.

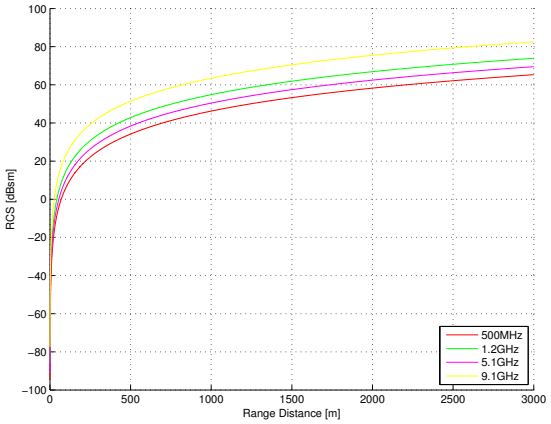

Figure 6. Minimum RCS detectable considering $BW = 120MHz$ and $SNR = 10dB$.

4. Simulator Architecture

Considering what has been detailed previously, a simulator of a FMCW radar systems developed with an USRP systems has been designed. This simulator essentially emulates a X300/X310 device equipped with a UBX 10-6000 MHz Rx/Tx daughterboard. Despite the hardware systems operates up to $6GHz$, we have also changed the necessary parameters for the simulator to be able to operate also at $9.1GHz$. The complete simulator has been developed as a Matlab Simulink model, which details can be observed in Fig. 12. In the following, we will detail each stage of the simulator and its different parameters.

4.1. Transmit Chain

In transmission, we will consider a chirp signal with $BW = 20MHz$ as later on we will simulate a detection of a target located at $500m$ away from the radar. Also, we will consider that the system will operate at P-band at $0.5GHz$.

The period of the chirp Signal T_p is established at $20\mu s$, limiting the maximum range at $3Km$. Since the FPGA has a streaming bandwidth of $200MS/s$, the chirp signal is shifted to $20 - 40MHz$ in order to have from 5 to 10 samples per period.

After the previous process, the real I/Q signals corresponding to the chirp are generated. The I/Q chirp signals are modulated using a sine wave signal of $20MHz$, obtaining at the output a $20MHz$ bandwidth signal located between $40 - 60MHz$, with 3.33 and 5 samples per period, respectively. After this step, the signal is interpolated by a factor of 4 to arrive to the to $800MS/s$ sampling frequency of the DAC. Before to go through the DAC process, the signals are up converted in the DUC to the range $60 - 80MHz$. Then, the signals is converted to the analog domain.

At this point, we have an analog signal in the range $60 - 80MHz$. Then, this signal is up converted in the front-

end to the desired carried frequency, in this case $0.5GHz$. Finally, we have also included different blocks adjusting the transmitted power and the gains of the transmitting antenna. For example, at $0.5GHz$, the signal must be have a power of $20dBm$. In this case, it was considered that the signal has an output power of $22dBm$, corresponding to $0.1584W$. Adding to this value the antenna gain in transmission, $6dB$, a signal of $28dBm$ is transmitted, which corresponds to a linear value of $0.63W$.

4.2. Propagation and Target Effects

As it can be observed in Fig. 12, we have also considered the effects of time delay, atmosphere attenuation and RCS of a trihedral corner reflector with a side of $2.41m$ located at $500m$ away from the radar.

4.3. Reception Chain

In reception, the signal follows almost the same path as in transmitting chain. The received signal by the antenna is first down converted to the $80MHz$ range, performing also the I/Q conversion. Then the signal goes through the ADC considering a sampling frequency of $200MS/s$. After this process, the signals go through the DDC blocks leading to a signal in the desired range of $0 - 20MHz$.

At this point of the process, that is, with the received signals in baseband, we perform the mixing process with the transmitting signal in order to obtain a signal which frequency is proportional to the distance of the target. As it can be observed, the scheme simulated in Fig. 12 is different from the initial scheme shown in Fig. 1, where the mixing process is performed at RF level. When addressing the design of the simulator we considered this architecture to avoid the introduction of external RF components.

5. Simualtion Results

The simulator designed in the previous section, is now tested to determine the detection performances of a $2.41m$ trihedral located $500m$ away from the radar. For this purpose, we consider a chirp signal where $BW = 20MHz$. First of all, we will consider the detection performances for the system operating at $0.5GHz$, where Fig. 8 shows the mixed signal f_b.

Considering a target located at $500m$, Table 3 shows the theoretical values of the signal f_b. Table 4 shows the parameters estimated from the received signal obtained with the simulator. As it can be observed, when operating at $0.5GHz$, the detection parameters are very close to the theoretical ones.

The previous results need to carefully detailed as these are obtained after a calibration process. As it can be deduced, a FMCW radar determines the distance of a target from the beat frequency f_b, which is proportional to the round-trip delay Δ_r. As indicated in Fig. 1, when the mixing procedure is performed at RF level, the detection is correct. Nevertheless, in the proposed simulator, the mixing process is performed at baseband, after the signal has gone through all the receiving chain. Consequently, any delay introduced by the receiving chain, will introduce a location error. For instance, in the proposed simulator we have observed a delay of $0.35\mu s$ producing a $f_b = 7.42MHz$ for $f_0 = 0.5GHz$. This system delay needs to be calibrated to avoid errors in location. Then, the results in Table 3 have considered this correction.

Table 3. Theoretical parameters of the received signal for a target located at $500m$.

f_b [MHz]	6.66
r_0 [m]	500
Δr [m]	9
Δf_{b-3dB} [KHz]	64

Table 4. Simulated result parameters of the received signal for a target located at $500m$.

f_0 [GHz]	0.5	1.2	5.2	9.1
f_b [MHz]	6.641	6.641	6.641	6.641
r_0 [m]	498	498	498	498
Δr [m]	9	10.7	14.5	17.2
Δf_{b-3dB} [KHz]	64	71.3	96.67	114.67

As indicated in Section 2, we also want the radar to operate at additional carrier frequencies f_0. Table 4 presents also the simulated results for 1.2, 5.2 and $9.1GHz$, where Fig. 9, 10 and 11 detail the spectrum of the detected signals, respectively.

.

6. Conclusions

This work details the implementation of a FMCW radar systems with a Ettus X300/X310 device equipped with a UBX 10-6000 MHz Rx/Tx daughterboard. In particular, we have designed a simulator in order to determine the expected performances of the radar. From the different simulation results, one may expect that the proposed radar system would achieve the necessary performances to be operational, at the same level of most GBSAR sensors developed nowadays. In particular, a range up to $3Km$ and a spatial resolution below $10m$ could be expected. In addition, the system could operate in all the frequency range of the SDR equipment. In addition, simulations beyond the limit

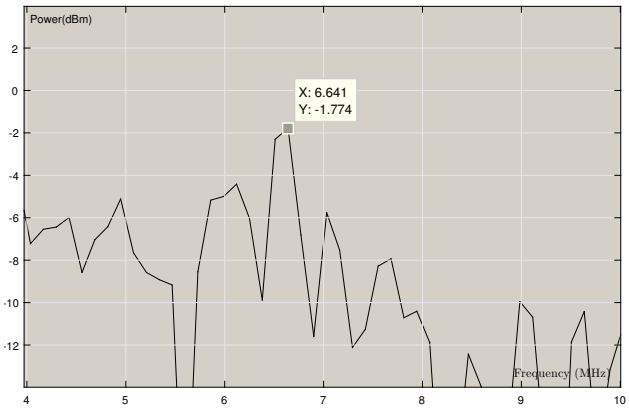

Figure 8. Spectrum of f_b when operating at $0.5GHz$.

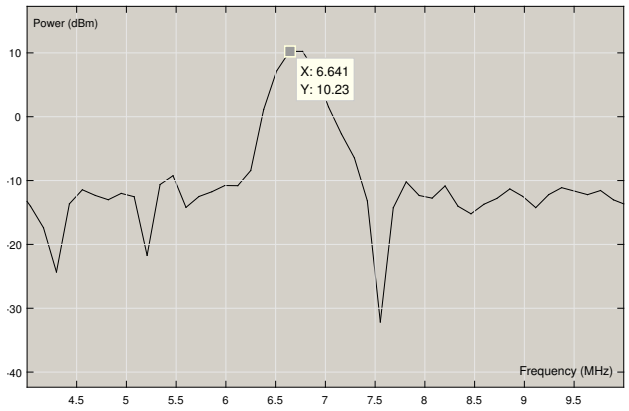

Figure 10. Spectrum of f_b when operating at $5.2GHz$.

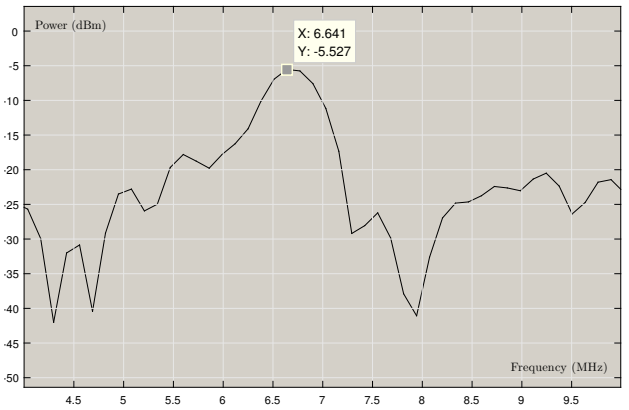

Figure 9. Spectrum of f_b when operating at $1.2GHz$.

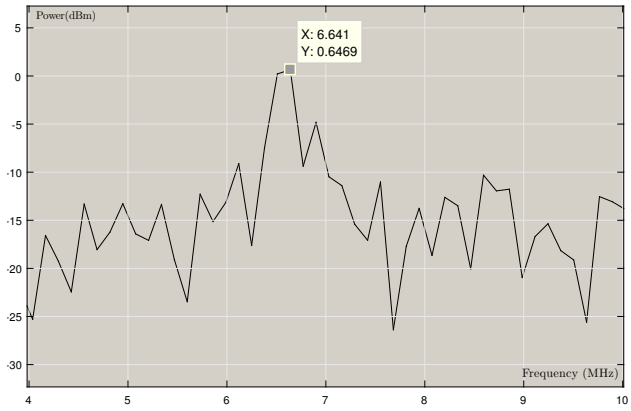

Figure 11. Spectrum of f_b when operating at $9.1GHz$.

of $6GHz$ have been conducted. From a practical point of view, this extended frequency range could be achieved with an external RF front end.

The simulator designed in this work does not pretend to be as accurate as possible. Nevertheless, it was designed in order to determine the potentialities of developing a FMCW radar system based on a SDR. In addition, the second purpose was to study the different architectures to achieve the functionalities of a FMCW radar. From this point of view, the most important stage of a FMCW radar system is the mixing block, that normally is performed at RF level. In this work, we have considered the mixing process at base band in order to exploit all the potentialities of the SDR technology. Nevertheless, this architecture presents two main drawbacks. Fist of all, the delay introduced by the system needs to be known very accurately in order to calibrate it if necessary. If not considered, or wrongly corrected, it would lead to location errors. The second drawback has to deal with the digitalization process of the received signal. Considering the mixing process at base band means that the digitalization process needs to digitalize a high bandwidth signal, that in some cases is in the limits of the digitalization process. The alternative that we would propose, as a main conclusion, is to digitalize the beat signal f_b as it is characterized by a much lower bandwidth. Consequently, the digitalization process would not operate at the limit of its capabilities.

The way to solve the previous two drawbacks is to develop an external RF block to perform the mixing process. With this alternative, the delays of the signal in the receiving chain do not longer introduce location errors and the digitalization process would be able to cope with the bandwidth of the beat frequency, and therefore leading to a much reliable digitalization.

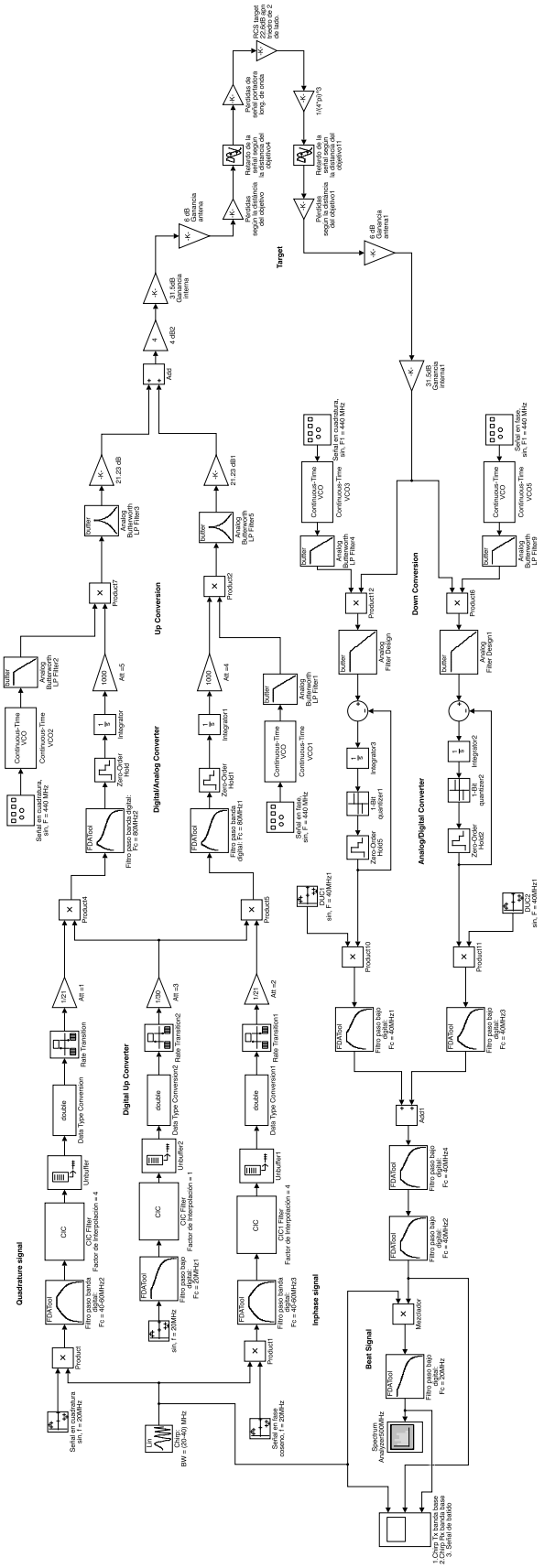

Figure 12. Matlab Simulink scheme of the simulated FMCW radar employing a SDR system.

7. Acknowledgements

This work has been supported by the project TIN2014-55413-C2-1-P, funded by the Spanish MICINN funds.

References

A., Aguasca, Broquetas, A., Mallorqui, J., and Fabregas, X. A solid state l to x-band flexible ground-based SAR system for continuous monitoring applications. In *Proceedings IGARSS*, pp. 757–760, Anchorage, USA, 2004.

Bamler, R., Adam, N., Davidson, G. W., and Just, D. Noise-induced slope distorsin in 2-d phase unwrapping by linear estimators with application to SAR interferometry. *Geoscience and Remote Sensing, IEEE Transactions on*, 36(3):913–921, May 1998.

Cloude, S. R. and Papathanassiou, K. P. Polarimetric SAR interferometry. *Geoscience and Remote Sensing, IEEE Transactions on*, 36(5):1551–1565, September 1998.

Cloude, S.R. and Pottier, E. A review of target decomposition theorems in radar polarimetry. *Geoscience and Remote Sensing, IEEE Transactions on*, 34(2):498–518, March 1996. doi: 10.1109/36.485127.

Curlander, J. C. and McDonough, R. N. *Synthetic Aperture Radar: Systems and Signal Processing*. John Wiley & Sons, Inc., New York, USA, 1991.

Elsner, J., Braun, M., Nagel, St., Nagaraj, K., and Jondral, F. Wireless networks in-the-loop: software radio as the enabler. In *Software Defined Radio Forum Technical Conference*, 2009.

Rudolf, H., Leva, D., Tarchi, D., and Sieber. A mobile and versatile SAR system. In *Proceeding of IGARSS*, volume 1, pp. 592–594, Hamburg, Germany, 1999.

Tarchi, D. interferometry for structural changes detection: A demonstration test on a dam. In *Proceeding of IGARSS*, volume 3, pp. 1522–1524, Hamburg, Germany, 1999.

Ulaby, F. T. and Elachi, C. *Radar Polarimetry for Geoscience Applications*. Artech House, Norwood, MA, 1990.